Brain Topogr (2013) 26:247–263
DOI 10.1007/s10548-012-0226-1

ORIGINAL PAPER

Processing of Coherent Visual Motion in Topographically Organized Visual Areas in Human Cerebral Cortex

Randolph F. Helfrich · Hubertus G.T. Becker · Thomas Haarmeier

Received: 6 February 2012 / Accepted: 28 March 2012 / Published online: 19 April 2012

Abstract Recent imaging studies in human subjects have demonstrated representations of global visual motion in medial parieto-occipital cortex (area V6) and posterior parietal cortex, the latter containing at least seven topographically organized areas along the intraparietal sulcus (IPS0–IPS5, SPL1). In this fMRI study we used topographic mapping procedures to delineate a total of 18 visual areas in human cerebral cortex and tested their responsiveness to coherent visual motion under conditions of controlled attention and fixation. Preferences for coherent visual motion as compared to motion noise as well as hemispheric asymmetries were assessed for contralateral, ipsilateral, and bilateral visual motion presentations. Except for areas V1–V4 and IPS3-5, all other areas showed stronger responses to coherent motion with the most significant activations found in V6, followed by MT/MST, V3A, IPS0-2 and SPL1. Hemispheric differences were negligible altogether suggesting that asymmetries in parietal cortex observed in cognitive tasks do not reflect differences in basic visual response properties. Interestingly, areas V6, MST, V3A, and areas along the intraparietal sulcus showed specific representations of coherent visual motion not only when presented in the hemifield primarily covered by the given visual representation but also when presented in the ipsilateral visual field. This finding suggests that coherent motion induces a switch in spatial representation in specialized motion areas from contralateral to full-field coding.

Keywords fMRI · Visual motion processing · V6 · MST · Intraparietal sulcus · Hemispheric asymmetries

Abbreviations

ANOVA	Analysis of variance
BOLD	blood oxygen level-dependent
EPI	Echo planar imaging
fMRI	Functional magnetic resonance imaging
IPS	Intraparietal sulcus
LOS/LOC	Lateral occipital sulcus/complex
MST	Medial superior temporal area
MT	Middle temporal area
MT+ complex	Middle temporal complex
pITS	Posterior part of the inferior temporal sulcus
POIPS	Parieto-occipital intraparietal sulcus
PSC	Percent signal change
ROI	Region of interest
SPL	Superior parietal lobe
TOS	Transverse occipital sulcus
VIP	Ventral intraparietal area

Introduction

The cortical processing of visual motion has been explored extensively in the last decades ever since direction-sensitive neurons in the temporal lobe of monkeys were

R. F. Helfrich · T. Haarmeier (✉)
Department of Neurology, RWTH Aachen University, Pauwelsstraße 30, 52074 Aachen, Germany
e-mail: thaarmeier@ukaachen.de

R. F. Helfrich · H. G.T.Becker
Department of Cognitive Neurology, Hertie Institute for Clinical Brain Research, University of Tübingen, 72076 Tübingen, Germany

R. F. Helfrich · H. G.T.Becker
Department of General Neurology, Hertie Institute for Clinical Brain Research, University of Tübingen, 72076 Tübingen, Germany

discovered (Allman and Kaas 1971; Desimone and Ungerleider 1986; Dubner and Zeki 1971; Maunsell and van Essen 1983). Until recently, studies in humans have largely concentrated on the human homologue of macaque area MT/V5, often referred to as the human MT+ complex located in the ascending limb of the inferior temporal sulcus (Amano et al. 2009; Becker et al. 2008; Born and Bradley 2005; Dumoulin et al. 2000; Huk et al. 2002; McKeefry et al. 1997; Tootell et al. 1995; Wall et al. 2008). While the essential role of area MT and its human homolog in visual motion processing is undisputed, several more recent studies have revealed further and distinct cortical areas involved. These include the posterior parietal lobe (Orban et al. 2006; Sunaert et al. 1999; Vanduffel et al. 2001), areas in the lateral occipital cortex (Braddick et al. 2001; Sunaert et al. 1999; Van Oostende et al. 1997), and the parieto-occipital junction (Fattori et al. 2009; Pitzalis et al. 2010; von Pfostl et al. 2009). More specifically, areas located in the intraparietal and the medial parieto-occipital sulcus have been implicated in visual motion processing since recent imaging studies in humans have demonstrated robust responses to global visual motion as opposed to motion noise in these areas (Cardin and Smith 2010; Evangeliou et al. 2009; Fattori et al. 2009; Konen and Kastner 2008; Pitzalis et al. 2010).

Formerly, the human intraparietal sulcus (IPS) has often been treated as consisting of either a single region or two subregions, i.e., the inferior and superior IPS. According to recent fMRI studies (Konen and Kastner 2008; Sheremata et al. 2010) exploiting the advantages of topographical mapping (Engel et al. 1994; Sereno et al. 2001) the medial/superior bank of the human IPS is by no means a uniform area but rather forms a continuous band of at least seven topographically organized parietal areas that can be differentiated also on the basis of other response properties related e.g. to eye movements, attention, or working memory (for a recent review see Silver and Kastner 2009). All the seven topographical areas showed motion-selective responses to planar, circular, and radial optic flow patterns in an fMR adaptation paradigm (Konen and Kastner 2008).

Another brain region to be considered a core element of the visual motion system is area V6 located in the medial parieto-occipital cortex and termed ‘the medial motion area’ by the authors of a recent fMRI study (Pitzalis et al. 2010). As demonstrated by numerous studies of the Galletti lab, V6 has a clear retinotopic organization in the macaque, which represents the contralateral hemifield. A peculiarity of V6 is its lack of a particular emphasis of the foveal representation so typical of other early visual areas. The majority of its cells are direction selective. Adjacent area V6A, which is not yet completely defined in human cortex, has no obvious retinotopic organization and fewer neurons are visually responsive albeit again prefer motion stimuli. It has been suggested that macaque V6 and V6A have a pivotal role in providing visual motion information to the motor system (Fattori et al. 1992; Galletti et al. 1991; Galletti et al. 1996; Galletti et al. 1999a; Galletti et al. 1999b). In humans, V6 has been identified using wide-field retinotopic mapping (Pitzalis et al. 2006). With macaque V6 it shares its retinotopic organization again providing a complete representation of the contralateral hemifield. Recent fMRI studies have shown that human V6 is a prototypical motion area, responding much more strongly to coherent than incoherent motion and, beyond, preferring flow field stimuli that truly simulate ego-motion (Cardin and Smith 2010; Pitzalis et al. 2010).

The goal of the present fMRI study was to further characterize the different areas of human visual cortex that have been implicated in the analysis of global visual motion. To this end, we used retinotopic mapping procedures (Engel et al. 1994; Sereno et al. 1995; Sereno et al. 2001; Swisher et al. 2007) in order to first delineate the different regions including, among others, IPS and V6 on a single subject basis and then compared the responses to coherent visual motion with those to motion noise. The study was further designed to address the following questions. (i) Visual motion stimuli were presented in the periphery, while subjects performed a demanding discrimination task at fixation (Konen and Kastner 2008). This approach allowed us to test, whether the preference of V6 or other areas for coherent motion as compared to noise stimuli would survive control for possible attentional differences between conditions. (ii) Since the parietal cortex is known to be involved in cognitive control processes that can exhibit significant hemispheric asymmetries (Posner and Petersen 1990), we compared responses between hemispheres, again under conditions of invariant attention and controlled fixation. (iii) While V6 and areas in the parietal cortex such as VIP have been suggested to play a functional role in the analysis of optic flow stimuli and, thus, the computation of ego-motion, their specific contribution may be limited by the fact that their visual representation might be confined to the contralateral visual hemifield. A valid computation of ego-motion based on optic flow information, however, should integrate visual motion information across the entire visual world. Against this background, we decided to analyze the responses to coherent visual motion to ipsilateral stimuli.

In summary, we present evidence that besides MT and MST also other areas represent coherent visual motion under conditions of controlled fixation and attentional demands, foremost areas V6, V3A, and areas in the IPS, in particular IPS0-2 and SPL1. Hemispheric asymmetries were negligible altogether suggesting that asymmetries in parietal cortex observed in cognitive tasks do not reflect differences in basic visual response properties. Finally,

areas V6, MST, V3A, and IPS0 revealed robust representations of coherent visual motion not only when presented in the hemifield covered by the given visual representation but also when presented in the ipsilateral visual field. These findings suggest that coherent motion induces a switch in spatial representation in specialized motion areas from contralateral to full-field coding.

Materials and Methods

Participants

Five healthy male subjects, all aged 23 years, participated in this study, including one of the authors (RFH). All subjects were right-handed with a laterality quotient of 81 ± 12 % (mean ± standard deviation) (Oldfield 1971). All of them had normal or corrected to normal vision. The experiments were approved by the local ethics committee at the medical faculty of the University of Tübingen and all subjects gave their written informed consent according to the Declaration of Helsinki. The naïve volunteers were paid for their participation.

Visual Stimuli

Stimulus generation and data acquisition were controlled by the open source nrec measurement system (http://nrec.neurologie.uni-tuebingen.de, created by F. Bunjes, J. Gukelberger et. al.) running on an IBM PC-compatible Pentium class computer. Visual stimuli were rendered in OpenGL and presented on a NEC GT 950 projector at resolution of 1024 × 768 pixels with a refresh rate of 60 Hz. The subjects viewed the projection screen behind the scanner through a mirror system attached to the head coil placed approximately 10 cm in front of their eyes which led to a field of view of almost 40° in the horizontal dimension and 20° in the vertical dimension. During the entire experiments the subjects were asked to maintain fixation on the central fixation point (diameter of 8.6 arc min). Attention was controlled by changing the color of the fixation point, randomly chosen out of six colors (red, yellow, blue, green, magenta, white), at a rate of 2 Hz in all experiments including the retinotopic mapping procedures. The participants had to count how often the fixation point turned blue and report the result verbally after each run (Wall et al. 2008). This task was introduced in order to keep attention stable and to minimize modulations in attention such as potentially resulting from different motion stimuli. It has been used previously by different groups (e.g. Larsson et al. 2006, Wall et al. 2008) and has also been demonstrated to be effective in eliminating effects of attentional modulation (Wall et al. 2008).

Retinotopic Mapping

The visual field maps were measured using phase-encoded stimuli techniques (DeYoe et al. 1996; Engel et al. 1994; Sereno et al. 1995; Wandell et al. 2007). The stimuli were extended to the edges of the screen. The stimulus for polar angle mapping was a monochromatic radial checkerboard with a radius of 10° reversing between "light" and "dark" at 8 Hz flicker frequency (Fox and Raichle 1985) and moving clockwise or counter-clockwise at a speed of 15°/sec (or 3.75°/sec during more detailed mapping). For eccentricity mapping the checkerboard was presented as expanding or contracting rings with a maximum outer radius of 10°. All subjects participated in at least four repetitions of every condition, each lasting 240 s (or 816 s during more detailed mapping) (Swisher et al. 2007). In total, each subject participated at least 1 h in this mapping procedure in order to increase the signal-to-noise ratio (Swisher et al. 2007).

Localizing and Disentangling the MT+ complex

Area V5/MT+ was identified using the motion stimulus as a functional localizer which has been shown to allow for a reliable separation of two functionally different subregions, i.e., areas we will refer to as MT and MST (Amano et al. 2009; Becker et al. 2008; Huk et al. 2002). Areas V5/MT+, MT and MST were identified by contrasting responses induced by coherent and incoherent motion to those obtained from the stationary control condition. The MT+ complex was defined by responses in the posterior part of the inferior temporal sulcus (pITS) induced by contralateral visual motion. Specifically, it was delineated as the cluster of contiguous voxels lying in the immediate neighborhood of the pITS and showing significantly stronger responses for the coherent and incoherent motion conditions as compared to the stationary pattern. Based on the large receptive fields of MSTd neurons in the macaque, which commonly cover also parts of the ipsilateral visual field, the human homolog of area MST was defined by all contiguous voxels within the hMT+ complex which were significantly active during ipsilateral motion stimulation (Becker et al. 2008; Desimone and Ungerleider 1986; Dukelow et al. 2001; Huk et al. 2002; Smith et al. 1998; Wall et al. 2008). Subtraction of the voxels assigned to MST from the MT+ complex isolated area MT. Thus, area MT only contained the voxels of the MT+ complex which were active during contralateral, but not during ipsilateral stimulation. In order to further improve separation of the two regions, voxels in hMT+ located anterior to the median axial coordinate of area hMST were not considered for MT. Note that preferences for coherent motion were analyzed after defining the ROIs but were not used beforehand to separate MT from MST.

Motion Coherence Stimuli

The stimulus consisted of rectangular random dot patterns with white dots on a dark background. The patterns were extended to the edges of the screen resulting in a maximum field of view of almost 40° in the horizontal and 20° in the vertical direction. The central visual area was not stimulated. Specifically, the inner borders of the rectangular dot field were set to 3° in horizontal direction. Each dot had a diameter of 8.6 arc min and moved at 6°/sec. They all had a limited lifetime of 1,000 ms (Becker et al. 2008), before disappearing and reappearing at a new random location. The dot density was 6 dots/degree^2 throughout all trials. In a 'coherent motion condition' the motion direction was the same for all dots. In the second condition, the 'incoherent motion condition', the dots moved independently in all possible directions. During the third condition, a stationary random dot pattern was presented with a limited dot lifetime of 1,000 ms as in the motion conditions. This 'stationary condition' served as the baseline. During both motion conditions, motion direction was changed every 2 sec either clockwise or counter-clockwise in steps of 60°. Each condition was presented for 12 sec.

One cycle followed a sequence of stationary pattern, incoherent motion, stationary pattern, and coherent motion pattern with an overall length of 48 sec. Every trial consisted of eight cycles and was terminated with a stationary pattern. Thus, each trial lasted 396 sec. Motion stimuli were presented in three different experiments differing with respect to the visual field being stimulated. Specifically, stimuli were presented either in the left visual hemifield, the right hemifield or simultaneously in both visual fields. Each subject completed five repetitions of each experiment, leading to an overall of 15 trials per subject.

Data Acquisition

Imaging Data

Images were acquired with a three Tesla whole-body MR scanner (*Magnetom Trio, A Tim System, Siemens Medical Solutions, Erlangen, Germany*) using a 12-channel phased-array head coil. Every subject participated in at least three scanning sessions. During each session, a high-resolution three-dimensional anatomical scan with a modified driven equilibrium Fourier transform (MDEFT) sequence (Deichmann et al. 2004) of the brain was acquired (TR: 10.55 ms, TE: 3.14 ms, TI: 680 ms, flip angle: 22°, voxel size: 1 × 1 × 1 mm^3, 176 contiguous axial slices, FOV: 256 mm).

Functional images were taken with an echo planar imaging (epi) sequence (TR: 3.0 sec, TE: 66 ms, flip angle: 90°, voxel size: 2.5 × 2.5 × 2.5 mm, 45 slices, FOV: 195 mm).

Eye-Tracking Data

In order to control fixation the eye position was recorded in all trials with an MR-compatible infrared camera (Sensomotoric Instruments, Teltow, Germany). The horizontal and vertical positions of one eye were extracted from the video signal at a rate of 60 Hz and stored for off-line analysis after analog-to-digital conversion.

Data Analysis

Imaging Data

Anatomical and functional images were analyzed using BrainVoyager QX Version 1.8.6 (Brain Innovation, Maastricht, The Netherlands).

The anatomical images from each subject were corrected for inhomogeneity and then averaged with further anatomical measurements of the same subject to increase the quality of the anatomical data for segmentation and further processing. Then they were segmented at the boundary of the grey and white matter and inflated, cut along the calcarine sulcus and flattened to a 2D-shape in order to define the ROIs (Goebel et al. 1998).

The functional images were preprocessed with slice scan time correction (using trilinear/sinc interpolation), linear trend removal, temporal high-pass filtering, three-dimensional motion correction and were interpolated to a spatial resolution of 2 × 2 × 2 mm^3. Anatomical and functional data were co-registered to the individual anatomy with SPM2 (Wellcome Department of Cognitive Neurology, London, UK) implemented in MATLAB (Mathworks Inc., Natick, MA, USA) with the scanner's position parameters and manual adjustment afterwards. All data were transformed in standard space according to the atlas of Talairach and Tournoux (1988).

For both hemispheres of each subject the regions of interest were selected based on the retinotopic mapping by fitting a model of a travelling-wave to the time-course of the stimulus. Moreover, the hemodynamic response could be matched to the position of the stimulus in the visual field (DeYoe et al. 1996; Engel et al. 1994; Sereno et al. 1995). The boundaries of the visual field maps were defined as the reversals in the direction of phase change. All ROIs were drawn manually on a flattened anatomy in Talairach space on the basis of these boundaries. Only the human MT+ complex, comprising areas hMT and hMST, was defined on the basis of the visual motion stimulus, which served as a specific localizer based on a general linear model (Becker et al. 2008; Dukelow et al. 2001; Huk et al. 2002; Smith et al. 2006).

For the further analysis of the ROIs, the time-courses of the functional scans were extracted by averaging the data

of every condition of every subject separately. The BOLD percent signal changes for the coherent and incoherent motion conditions were generated by defining the 'stationary random dot pattern condition' as baseline. For statistical analysis of significant differences between the coherent and incoherent motion conditions, the BOLD percent signal changes were subjected to an ANOVA (analysis of variance) with repeated measures. In order to correct for multiple comparisons, we initially used 3-way repeated measures ANOVAs to reveal a significant influence of the factor 'region of interest'. We continued with post hoc 2-way repeated measures ANOVAs for all regions of interest and evaluated the differences in BOLD percent signal changes by a post hoc two-tailed paired *t*-test. Differences between conditions for a given ROI as revealed by post hoc *t*-tests were considered significant only if the effect was replicated in the final experiment involving bilateral visual stimulation. Since the chance level for false positives within the same ROI was thus $0.05 \times 0.05 = 0.0025$, this criterion was equally restrictive as a Bonferroni correction ($p = 0.05/18$ areas $= 0.0028$). We further quantified the results by the effect sizes as defined by Cohen's *d* (Cohen 1988).

Eye-Tracking Data

The analysis of the eye tracking data was performed with in-house software based on MATLAB. The eye position signal was filtered at a cut-off frequency of 15 Hz. Eye blinks were detected through visual inspection and were removed via linear interpolation. For each trial the mean horizontal and vertical eye positions and their standard deviations were calculated separately for coherent, incoherent and stationary random dot patterns and finally tested for differences in the eye position using two-tailed paired *t*-test (Bonferroni-corrected).

Results

ROI Definitions

Phase-encoded retinotopic mapping procedures were used to identify previously described areas V1, V2, V3, V4, V3A, V3B, LO1, LO2, IPS0-5, SPL1 and V6 as specified in detail below. The retinotopic maps for standard and intensive mapping procedures (see "Materials and Methods") did not differ, although the application of larger stimuli during standard mapping (wedge size: 90°) simplified the identification of retinotopically organized regions with larger receptive fields. In contrast, smaller retinotopic stimuli such as used for intensive mapping (wedge size: 22.5°) provided a better discrimination effect at the borders of adjacent areas (Swisher et al. 2007; Wandell et al. 2007). The influence of the wedge size was diminished and the signal-to-noise ratio was increased by averaging over several repetitions of measurements as described in the "Materials and Methods". In the following, we assigned V1–V4 to the primary visual areas, areas IPS0-5 and SPL1 to the parietal areas and all other regions to the group of intermediate or gateway areas as suggested by Orban et al. (2006). Ventral and dorsal parts of areas V2 and V3, respectively, were pooled and treated as single ROIs.

Retinotopic Mapping, ROI Definitions

Figure 1 shows the location of the different visual areas in one representative subject. For the group of subjects, the mean coordinates of the ROIs (Talairach space) and the sizes of ROIs are given in Table 1. The areas V1–V3 were identified based on their anatomical topography around the calcarine sulcus and occipital pole. They share a confluent foveal representation and represent the upper contralateral quarter field on the ventral surface and the lower contralateral quarter field on the dorsal surface (DeYoe et al. 1996; Engel et al. 1994; Sereno et al. 1995). Ventral area V3 has also been referred to as area VP in the literature (Sereno et al. 2001). Human area V4 was localized in the fusiform gyrus and has been defined by its complete representation of the contralateral hemifield anterior to the ventral part of area V3 (Wade et al. 2002; Wandell et al. 2007). Area V3A (Braddick et al. 2001; Press et al. 2001; Tootell et al. 1997) beginning at the border of the dorsal portion of area V3 at the lower vertical meridian includes a complete representation of the contralateral hemifield. Area V3B is located dorsally and laterally to area V3A along the transverse occipital sulcus and is separated by a local minimum in the eccentricity map. It shares a discrete confluent foveal representation with area V3A (Press et al. 2001; Swisher et al. 2007) and also contains a complete hemifield representation (Press et al. 2001; Swisher et al. 2007). Therewith, we followed the definition of Press et al., though different definitions of the visual field maps of V3B have been suggested (Smith et al. 1998; Wall et al. 2008). The areas LO1 and LO2 were found anterior to the dorsal part of area V3 in the lateral occipital sulcus, with LO1 covering a hemifield from the lower to the upper vertical meridian and LO2 containing a hemifield starting at the upper vertical meridian adjacent to area LO1 (Larsson and Heeger 2006; Swisher et al. 2007). LO1 was separated from area V3B by its shared foveal representation with V1–3 (Larsson and Heeger 2006; Swisher et al. 2007; Kolster et al. 2010).

The parietal ROIs were separated into seven different regions starting with IPS0, formerly labeled V7 (Swisher et al. 2007; Wandell et al. 2007). Area IPS0 was identified being anterior to V3A and defined by a hemifield map starting at the upper vertical meridian (Press et al. 2001).

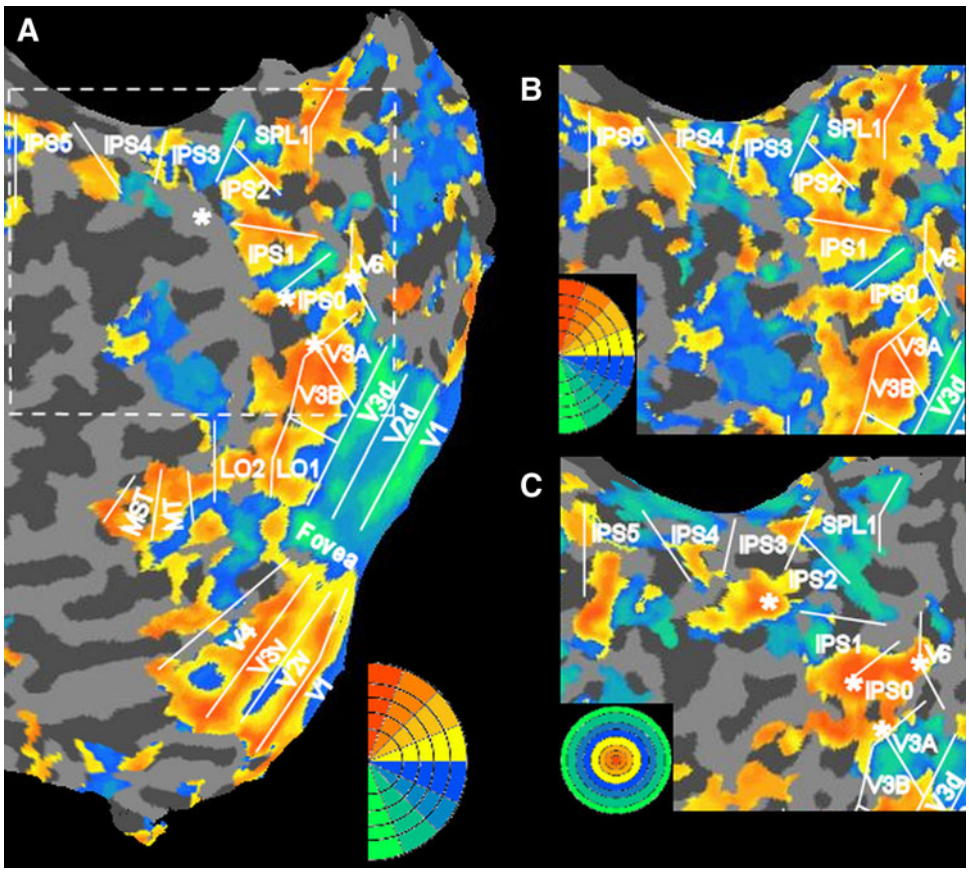

Fig. 1 **a** Overview: Visuotopic map on a flattened left hemisphere of one subject after angular mapping with a rotating wedge stimulus. *Green colors* represent the lower vertical meridian, *red colors* represent the upper vertical meridian and borders between *yellow* and *blue mark* the horizontal meridian in the contralateral hemifield (legend bottom center, radius = 10°). Only the MT+ complex with its subregions MT and MST was identified using the motion stimulus and their boundaries have been superimposed onto the retinotopic flat map. The area within the *dashed square* is demonstrated in more in detail in panels **b** and **c**. **b** Visuotopic field map of the area indicated in **a** using lower statistical threshold criteria ($r > 0.18$; **a**: $r > 0.22$) in order to demonstrate continuous field representations in the parietal areas. **c** Visuotopic field map on the flattened hemisphere after eccentricity mapping. The foveal representations are marked by an asterisk. We found shared foveal representations for V3A/B, IPS0/1 and IPS2/3 and a distinct foveal representation for V6. In addition, the angular mapping results are superimposed. Foveal representations are red, the outer eccentricity is blue/green (legend bottom left in 1C, radius 10°) (Color figure online)

IPS1 was found to share a confluent foveal representation with IPS0. Its hemifield representation begins at the lower vertical meridian. The hemifield representations along the intraparietal sulcus that follow in anterior direction were labeled in the order of their appearance as IPS2-5 (Konen and Kastner 2008; Swisher et al. 2007). IPS2 begins at the upper vertical meridian and shares a confluent foveal representation with IPS3 (Swisher et al. 2007), the latter beginning at the lower vertical meridian and also including a hemifield representation. IPS4 lies adjacent to IPS3 and covers a hemifield from the upper to the lower vertical meridian. We also observed a hemifield map of IPS5, a finding not consistently observed in the previous studies (Konen and Kastner 2008; Silver and Kastner 2009; Swisher et al. 2007). IPS5 was found to be situated anteriorly and laterally to area IPS4 and to extend towards the post-central sulcus. We found foveal representations for IPS4 and IPS5 lateral from the more peripheral responses. The boundaries of IPS5 were defined by the lower vertical meridian (at the border to IPS4) and the upper vertical meridian in the anterior direction (Konen and Kastner 2008). Areas IPS3-5 are rotated anterior-laterally relative to the posterior IPS0-2 maps. Swisher et al. (2007) pointed out that these maps can show substantial gaps or drop-outs. We found continuous representations when the statistical criteria were lowered (Fig. 1b). In addition to six intraparietal areas, we found a hemifield map branching off the intraparietal sulcus and extending into the superior parietal lobule, which comprised a hemifield from the lower to the upper vertical meridian. We believe this map to correspond to an area formerly labeled SPL1 (Konen and Kastner 2008). Area V6 was identified in the parieto-occipital

sulcus close to area V3A and IPS0 and was defined through an upper vertical meridian at the border to V3/V3A and a lower vertical meridian as its border to the IPS. The mean Talairach coordinates of all the different areas defined along this protocol were in excellent accordance with previous studies (Table 1; Swisher et al. 2007; Konen and Kastner 2008). This was also true for areas MT and MST localized by means of the motion stimulus (Becker et al. 2008; Dukelow et al. 2001; Huk et al. 2002).

Responses to Coherent and Incoherent Motion: Contralateral Stimulation

After the definition of the ROIs and the extraction of the BOLD percent signal changes for every region in both hemispheres of all subjects and under all stimulation conditions (stimulation of the left visual hemifield, right hemifield, and both hemifields), separately, we considered the regions of both hemispheres and readout the ROIs for the different types of stimulation. Therefore, activations for the condition 'contralateral stimulation' included the ROIs of the left hemisphere after stimulation in the right visual field and the right hemisphere ROIs stimulated by motion in the left visual field. The stationary condition served as a baseline in all three stimulation conditions. Performing a repeated measures 3-way-ANOVA with the factors motion condition (coherent, incoherent), ROI, and hemisphere revealed a highly significant influence of the factor region of interest ($F_{1,19} = 17.18$, $p < 0.0005$). Then, we continued using 2-way-ANOVAs with repeated measures for every ROI. In particular, we considered the factors motion condition and hemisphere in order not only to localize the processing of coherent visual motion, but also for detecting differences between the two hemispheres. Table 2 provides the summary of this analysis and also includes post hoc two-tailed paired *t*-tests and effect sizes. In order to correct for multiple comparisons, differences between motion conditions for a given ROI as revealed by post hoc *t*-tests were considered significant only if the effect was replicated in the later experiment involving bilateral visual stimulation (see "Materials and Methods").

Area V1 was the only region with a clear preference for incoherent as compared to coherent motion ($F_{1,12} = 22.95$, $p < 0.0005$), whereas V2, V3 and V4 were not preferring either of the two types of motion (V2: $F_{1,32} = 0.94$, $p > 0.05$; V3: $F_{1,32} = 1.12$, $p > 0.05$; V4: $F_{1,12} = 0.51$,

Table 1 Talairach coordinates and ROI sizes

	x (+/−)	y	z	ROI size (mm^3)
Primary visual areas				
V1	10 ± 4	−75 ± 5	2 ± 5	10986 ± 1550
V2	11 ± 4	−84 ± 4	−5 ± 4	6212 ± 266
V3	18 ± 4	−81 ± 4	−2 ± 6	5917 ± 399
V4	28 ± 4	−67 ± 4	−13 ± 3	2859 ± 393
Intermediate areas				
V3A	22 ± 5	−84 ± 3	21 ± 6	3111 ± 636
V3B	27 ± 3	−81 ± 7	13 ± 5	2772 ± 556
LO1	33 ± 3	−78 ± 3	7 ± 4	2601 ± 420
LO2	40 ± 4	−71 ± 3	5 ± 3	2708 ± 539
MT	46 ± 4	−63 ± 4	0 ± 4	2436 ± 1295
MST	44 ± 4	−65 ± 3	1 ± 5	1965 ± 572
V6	20 ± 5	−76 ± 6	31 ± 4	2895 ± 625
Intraparietal visual areas				
IPS0	28 ± 4	−74 ± 4	19 ± 7	5480 ± 582
IPS1	27 ± 3	−68 ± 6	25 ± 6	4853 ± 982
IPS2	24 ± 3	−64 ± 5	32 ± 6	4252 ± 959
IPS3	18 ± 3	−64 ± 5	39 ± 5	3980 ± 1268
IPS4	12 ± 6	−67 ± 4	43 ± 5	3390 ± 712
IPS5	16 ± 7	−63 ± 4	52 ± 2	3258 ± 714

Table 2 Comparison of responses to coherent and incoherent motion: contralateral stimulation

	T	*p*	*	*d*	SD
Primary visual areas					
V1	−4.27	0.0021	**	−1.99	0.39
V2	−0.86	0.4017		−0.29	0.21
V3	1.10	0.2846		0.49	0.17
V4	0.03	0.8569		0.27	0.12
Intermediate areas					
V3A	4.67	0.0012	**	1.71	0.17
V3B	3.77	0.0044	**	1.74	0.11
LO1	5.01	0.0007	***	1.18	0.12
LO2	2.83	0.0198	*	1.29	0.09
MT	7.10	0.0001	***	1.98	0.11
MST	4.73	0.0011	**	1.26	0.30
V6	8.10	<0.0001	***	3.88	0.14
Parietal Visual Areas					
IPS0	6.74	0.0001	***	2.48	0.07
IPS1	4.86	0.0009	**	1.84	0.07
IPS2	7.26	<0.0001	***	2.03	0.09
IPS3	3.62	0.0056		1.16	0.10
IPS4	3.54	0.0063		0.89	0.07
IPS5	4.78	0.0010		0.96	0.06
SPL1	4.91	0.0008	**	1.67	0.15

Statistical comparison of the BOLD responses induced by coherent and incoherent motion in all regions of interest after contralateral stimulation. *T*-values and *p*-values obtained from a two-tailed paired t-test, effect sizes given by Cohen's d, and pooled standard deviations of the BOLD percent signal changes (see Fig. 2). Asterisks indicate statistical level of significance: *<0.05; **<0.005; ***<0.0005; statistical significance is marked only if the effect was replicated in Experiment 3 involving bilateral stimulation

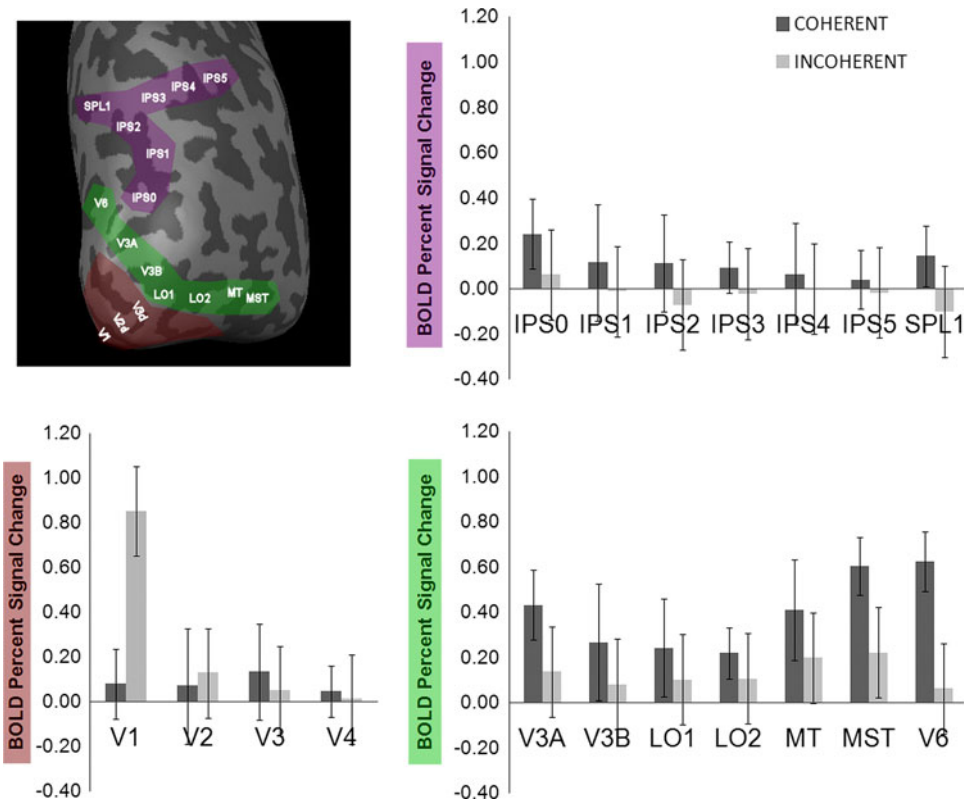

Fig. 2 Responses to coherent and incoherent motion observed for visual stimulation in the contralateral visual field. Means and standard deviations of BOLD percent signal change as compared to baseline (stationary random dot patterns). An inflated right hemisphere of one subject is presented for better orientation (Color figure online)

$p > 0.05$). For most of the other regions of interest the ANOVAs revealed a significantly stronger response to coherent visual motion. Especially, highest *t*-values and effect sizes were observed in areas V3A, LO1, MT and MST as parts of the MT+ complex, V6, and also in IPS0-2 and SPL1 (V3A: $F_{1,12} = 22.01$, $p < 0.0005$; LO1: $F_{1,12} = 5.01$, $p < 0.005$; MT: $F_{1,12} = 57.49$, $p < 0.0005$; MST: $F_{1,12} = 11.68$, $p < 0.005$; V6: $F_{1,12} = 72.72$, $p < 0.0005$; IPS0: $F_{1,12} = 30.82$, $p < 0.0005$; IPS1: $F_{1,12} = 19.57$, $p < 0.005$; IPS2: $F_{1,12} = 68.53$, $p < 0.0005$; SPL1: $F_{1,12} = 15.04$, $p < 0.005$; Table 2). There was also a trend for higher responses to coherent motion in areas IPS3-5 as compared to incoherent motion. Effect sizes, however, were overall small (Table 2). Further, the effects were not replicated in the bilateral stimulation experiment (see below) and, thus, not considered significant.

The area showing both highest *t*-values and effect sizes, and thus, the one showing the most robust preference to coherent motion was area V6. Interestingly, areas along the intraparietal sulcus showed a tendency for a slight decrease of the BOLD signal to incoherent motion which was not present in the other areas studied. The factor hemisphere seemed significant for area LO1 ($F_{1,12} = 13.22$, $p < 0.005$) revealing a stronger BOLD percent signal change in the right as compared to the left hemisphere. This difference, however, did not survive the experimental control involving bilateral stimulation. None of the other regions showed noticeable asymmetries.

Responses to Coherent and Incoherent Motion: Ipsilateral Stimulation

In this condition, testing responses to ipsilateral visual motion stimuli, again data of both hemispheres were considered: the ROIs of the left hemisphere stimulated by the motion stimulus in the left visual field and the ROIs of the right hemisphere with stimulus presentation in the right visual field. Results are summarized in Fig. 3 and Table 3.

As mentioned above, we performed a 3-way ANOVA with repeated measures first, which again revealed a strong influence of the factor ROI ($F_{1,19} = 15.31$, $p < 0.0005$). Consecutive 2-way repeated measures ANOVAs for all ROIs gave detailed information on preferences of coherent as compared to incoherent motion and hemisphere differences. Preferences for coherent motion were only observed in areas that had revealed the same preference during contralateral stimulation. Specifically, robust representations of coherent visual motion in the ipsilateral hemifield were observed in the areas MST and V6 (MST: $F_{1,12} = 17.64$, $p < 0.005$; V6: $F_{1,12} = 57.68$, $p < 0.0005$), whereas MT as the other part of the MT + complex did not show a significant preference for coherent versus incoherent motion in this condition (MT: $F_{1,12} = 0.13$, $p > 0.05$). Also the ROIs V3A, V3B and LO1 showed stronger responses to coherent visual motion (V3A: $F_{1,12} = 21.74$, $p < 0.005$; V3B: $F_{1,12} = 9.27$, $p < 0.05$; LO1: F1,12 = 7.00, $p < 0.05$), but LO2 did not (LO2: $F_{1,12} = 1.82$,

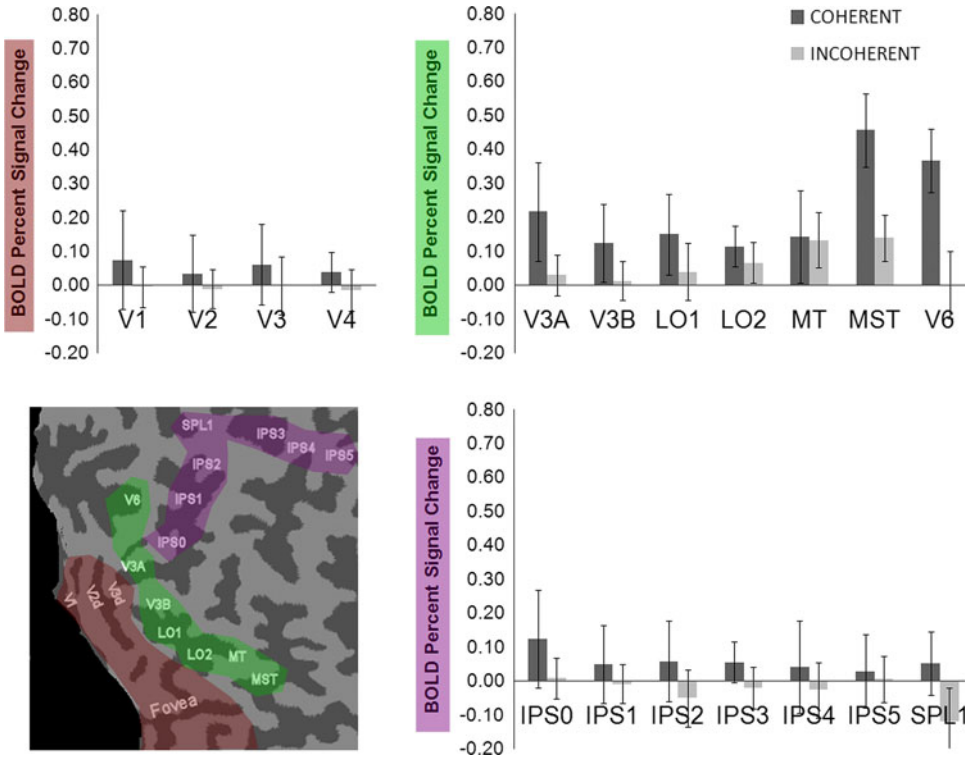

Fig. 3 Responses to coherent and incoherent motion observed for visual stimulation in the ipsilateral visual field. Means and standard deviations of BOLD percent signal change as compared to baseline (stationary random dot patterns). A flattened right hemisphere (same subject as in Fig. 2) is presented for better orientation. Same color conventions as in Fig. 2 (Color figure online)

Table 3 Comparison of responses to coherent and incoherent motion: ipsilateral stimulation

	T	*p*	*	*d*	*SD*
Primary visual areas					
V1	1.83	0.1009		0.72	0.11
V2	1.52	0.1458		0.50	0.09
V3	1.86	0.0779		0.61	0.10
V4	1.40	0.1964		0.89	0.06
Intermediate areas					
V3A	4.40	0.0017	**	1.67	0.11
V3B	2.75	0.0227	*	1.24	0.09
LO1	2.66	0.0259	*	1.15	0.10
LO2	1.31	0.2224		0.59	0.08
MT	0.55	0.5982		0.12	0.08
MST	4.09	0.0027	**	1.66	0.19
V6	7.42	<0.0001	***	3.44	0.11
Parietal visual areas					
IPS0	5.31	0.0005	***	2.13	0.05
IPS1	3.19	0.0111	*	1.04	0.06
IPS2	2.80	0.0206	*	1.04	0.10
IPS3	2.74	0.0227		0.86	0.09
IPS4	2.19	0.0562		0.81	0.08
IPS5	1.03	0.3302		0.41	0.06
SPL1	3.02	0.0145	*	1.18	0.15

Statistical comparison of the BOLD responses induced by coherent and incoherent motion in all regions of interest after ipsilateral stimulation. Same conventions as in Table 2. SD denotes pooled standard deviations of BOLD percent signal changes (see Fig. 3)

$p > 0.05$). Considering the intraparietal regions, we found significant differences between activations for coherent and incoherent motion in IPS0-2 and also in SPL1 (IPS0: $F_{1,12} = 23.57$, $p < 0.0005$; IPS1: $F_{1,12} = 6.17$, $p < 0.05$; IPS2: $F_{1,12} = 8.33$, $p < 0.05$; SPL1: $F_{1,12} = 10.57$, $p < 0.05$), whereas there was no statistically significant difference between the two motion conditions in IPS3-5 (IPS3: $F_{1,12} = 7.35$, $p < 0.05$, not replicated in the bilateral stimulation experiment; IPS4: $F_{1,12} = 4.59$, $p > 0.05$; IPS5: $F_{1,12} = 1.02$, $p > 0.05$). Again areas IPS1-4 and SPL1 showed a tendency for a slight decrease in response to incoherent motion stimuli. Notably, the areas showing significant responses to global visual motion in the ipsilateral visual field did not respond to ipsilateral stimulation during the angular mapping procedure. Figure 4 demonstrates the time-course for three of the ROIs in one of the subjects, revealing a strong response to contralateral stimulation (time 1–48 sec) but absent or even suppressed BOLD activations during ipsilateral stimulation (time 49–96 sec).

Responses in the primary visual areas V1–V4 were not reflecting coherent motion in the ipsilateral field (Fig. 3): comparison of the BOLD responses revealed no significant difference between the two motion conditions (V1: $F_{1,12} = 3.07$, $p > 0.05$; V2: $F_{1,12} = 2.27$, $p > 0.05$; V3: $F_{1,12} = 3.01$, $p > 0.05$; V4: $F_{1,12} = 2.98$, $p > 0.05$). With the single exception of area IPS0 which revealed higher activations for the right as compared to the left hemisphere ($F_{1,12} = 4.90$, $p < 0.05$), none of the ROIs considered

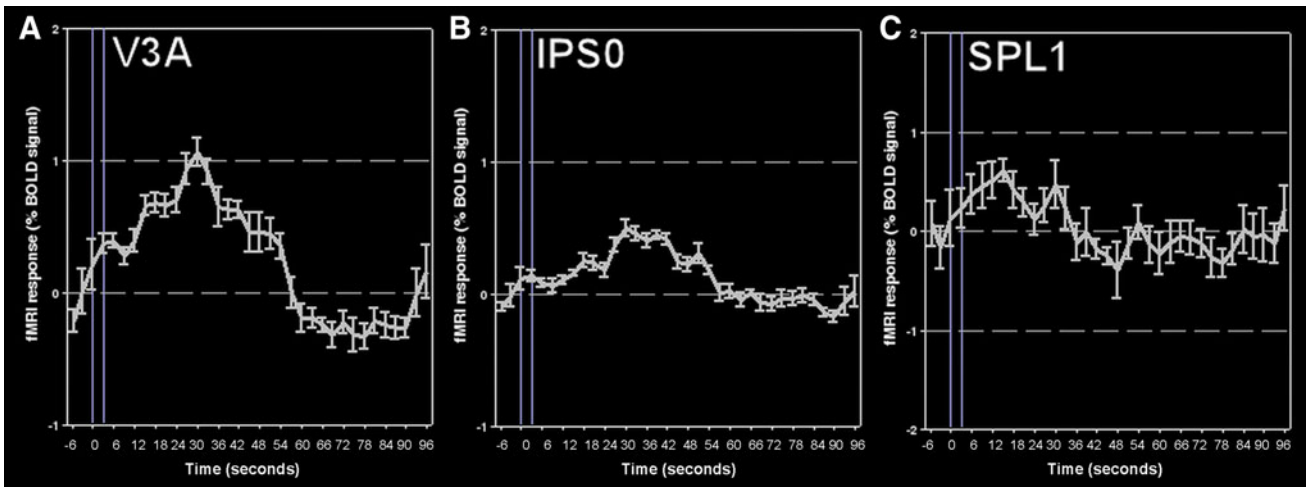

Fig. 4 Event-related time course of the BOLD responses observed in three different ROIs (**a–c**) during angular mapping (right hemisphere of one subject; mean BOLD percent signal change ± SEM). The x-axis spans a total of 96 sec representing one cycle of angular mapping. The wedge traverses the contralateral visual space during the first 48 sec and the ipsilateral visual field during the last 48 sec. In order to analyze the retinotopic mapping data, we used linear correlation maps and predicted the model of a travelling-wave, i.e. a boxcar function, as a reference derived from the whole MRI data volume. The time courses shown are the result of the temporal alignment of the given ROI signal to this reference function which also defines its baseline

showed any significant influence of the factor hemisphere. The asymmetry observed in IPS0 was not replicated in any of the two other experiments.

Coherent and Incoherent Motion at Bilateral Stimulation

For bilateral stimulation, the 3-way repeated measures ANOVA, analogous to the first two experiments, again revealed a strong influence of the factor ROI ($F_{1,19} = 16.07$, $p < 0.0005$). By the following 2-way repeated measures ANOVAs we obtained results that were highly congruent with the former two experiments (Fig. 5; Table 4). Only ROIs that had already shown influences of motion condition in the first two experiments showed similar effects under this condition. Similar to the first experiment employing contralateral stimuli alone, V1 revealed a strong and significant preference for incoherent visual motion ($F_{1,12} = 35.99$, $p < 0.0005$). Again, the areas V2–V4 did not differ in their BOLD signals for the two motion conditions (V2: $F_{1,12} = 3.06$, $p > 0.05$; V3: $F_{1,12} = 0.22$, $p > 0.05$; V4: $F_{1,12} = 0.40$, $p > 0.05$). All other ROIs except for IPS3-IPS5 showed a stronger activation to coherent as compared to incoherent motion. Areas with the highest t-values and effect sizes included V3A, MST, V6, and IPS0-IPS2 (V3A: $F_{1,12} = 13.05$, $p < 0.005$; MT: $F_{1,12} = 11.41$, $p < 0.0005$; MST: $F_{1,12} = 27.36$, $p < 0.0005$; V6: $F_{1,12} = 50.27$, $p < 0.0005$, IPS0: $F_{1,12} = 41.75$, $p < 0.0005$; IPS1: $F_{1,12} = 25.78$, $p < 0.0005$; IPS2: $F_{1,12} = 12.50$, $p < 0.005$). Like in both previous experiments, it was area V6 which showed the most specific response to coherent motion.

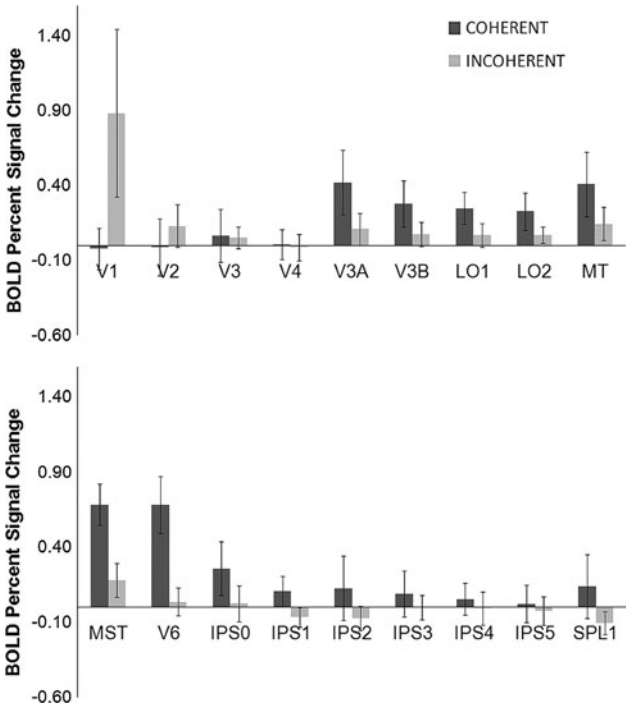

Fig. 5 Responses to coherent and incoherent motion observed for visual stimulation in both visual fields. Means and standard deviations of BOLD percent signal change as compared to baseline (stationary random dot patterns)

In V6 the response to incoherent motion was virtually absent. With respect to the intraparietal areas, the mean BOLD amplitudes of most of the ROIs trended to negative values for incoherent motion. The regions IPS0-2 in posterior parietal cortex and SPL1 ($F_{1,12} = 6.06$, $p < 0.05$) in the superior

Table 4 Comparison of responses to coherent and incoherent motion: bilateral stimulation

	T	*p*	*	*d*	*SD*
Primary visual areas					
V1	−4.52	0.0015	**	−2.22	0.41
V2	−1.70	0.1063		−0.85	0.17
V3	0.37	0.7137		0.10	0.14
V4	0.91	0.3866		0.19	0.10
Intermediate areas					
V3A	3.73	0.0047	**	1.84	0.17
V3B	3.29	0.0094	*	1.66	0.12
LO1	3.87	0.0038	**	1.92	0.09
LO2	3.24	0.0102	*	1.63	0.10
MT	2.98	0.0155	*	1.54	0.17
MST	5.06	0.0007	**	2.44	0.21
V6	6.83	0.0001	***	3.33	0.19
Parietal visual areas					
IPS0	7.73	0.0001	***	2.78	0.08
IPS1	4.77	0.0010	**	2.48	0.07
IPS2	3.20	0.0109	*	1.42	0.14
IPS3	1.50	0.1674		0.74	0.12
IPS4	1.42	0.1881		0.58	0.11
IPS5	1.08	0.3095		0.46	0.10
SPL1	2.23	0.0500	*	1.16	0.21

Statistical comparison of the BOLD responses induced by coherent and incoherent motion in all regions of interest after bilateral stimulation. Same conventions as in Table 2. SD denotes pooled standard deviations of BOLD percent signal changes (see Fig. 5)

parietal lobule showed stronger responses to coherent versus incoherent motion. In contrast BOLD responses of areas IPS3-5 did not differentiate between motion conditions (IPS3: $F_{1,12} = 2.85$, $p > 0.05$; IPS4: $F_{1,12} = 2.42$, $p > 0.05$; IPS5: $F_{1,12} = 1.55, p > 0.05$), thus not replicating the small effects in neighboring areas IPS3 and 5, which had been observed in the first experiments. The 2-way repeated measures ANOVA did not reveal any influences for the factor hemisphere in any of the regions of interest.

Comparison Between Cortical Hemispheres

As already indicated, differences between the two cortical hemispheres in coherent motion processing were overall small. For contralateral motion presentation, only LO1 revealed a small difference (factor hemisphere for LO1: $F_{1,12} = 13.22$, $p < 0.005$; Cohen's $d = 1.31$, SD = 0.11) with larger responses present in the right hemisphere. Figure 6 provides an overview of different ROIs for contralateral presentation of coherent motion. In the 'ipsilateral stimulation' condition, only IPS0 showed a tendency for an asymmetry (factor hemisphere for IPS0: $F_{1,12} = 4.90$, $p < 0.05$; Cohen's $d = 2.13$, SD = 0.05), revealing again a higher activation in the right hemisphere ROI. BOLD responses in LO1 were not significantly different during ipsilateral stimulation (factor hemisphere for LO1: $F_{1,12} = 1.11$, $p > 0.05$). For bilateral stimulation, no single ROI showed a significant hemispheric difference. In summary, in contrast to the robust representations of coherent visual motion that could be replicated applying bilateral stimulation, influences of the cortical hemispheres were close to chance level and could not be replicated.

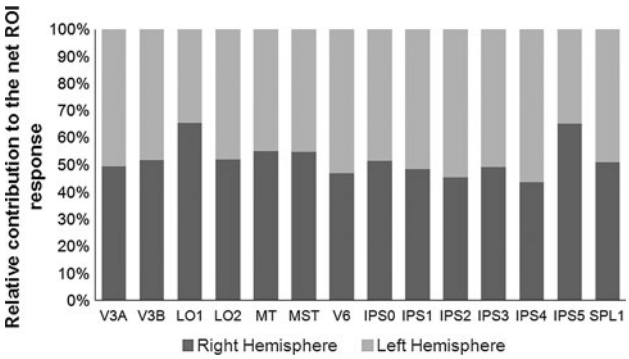

Fig. 6 Relative contributions of the right and the left hemisphere to the net activation of a given ROI induced by contralateral coherent motion where 100 % represent the sum of activations of both hemispheres. 50 % indicate identical responses in both hemispheres

Influences of Eye Movements and the Attention Task

Activity in many areas like the MT+ complex or in intraparietal regions is known to be modulated by eye movements and also attention (Andersen 1989; Astafiev et al. 2003; Dukelow et al. 2001; Haarmeier and Kammer 2010; Handel et al. 2008; Heide and Kompf 1998; Schluppeck et al. 2006; Tikhonov et al. 2004). Therefore, eye movements were recorded for fixation verification. In addition, we embedded a demanding attention task in the central fixation point. The subjects were instructed to count the number of specific color changes of the fixation spot which changed colors at a rate of 2 Hz. The average total count of events per trial was between 40 and 60 for retinotopic mapping procedures and between 60 and 110 for the motion trials. The subjects named the exact number of color changes in 28 % of all trials (42 % during retinotopic mapping, 12 % correct during motion trials). Figure 7 shows their overall performance during all the motion trials. As can be seen, the deviation of the reported color changes (per trial) from the correct number was small in the majority of trials. The task was difficult enough, however, to allow only a small fraction of trials to be answered correctly (12 %). The mean of the absolute value of the deviations was 3.0 ± 3.13.

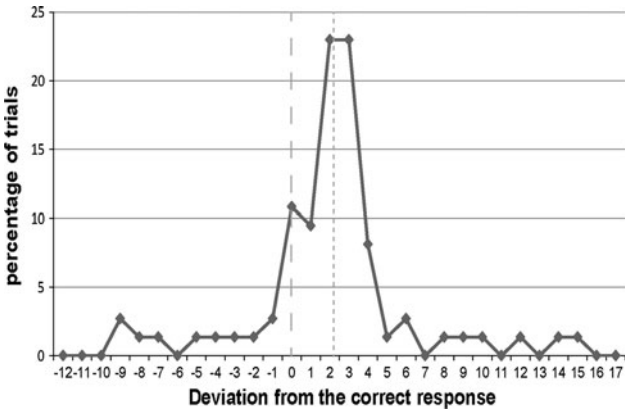

Fig. 7 Performance of the subjects in the attention task during the motion trials. Frequency of deviations of the reported number of color changes (per trial) from the correct number. The large dashed line at 0 represents trials with exact responses (no deviation). The distribution of responses is slightly shifted towards positive deviations peaking at around 2 and reflecting that subjects tended to slightly overestimate the number of color changes

Eye movement recordings could be performed and analyzed in most, i.e., 68 out of 75 measurements. Stable fixation was maintained by all subjects throughout the whole recording time as indicated by mean horizontal eye positions of 0.30° ± 0.94 during bilateral visual stimulation, 0.59° ± 0.13 during left stimulation, and −0.07° ± 0.08 during right stimulation (Fig. 8). The mean eye positions in vertical direction were −0.08° ± 0.12 during bilateral stimulation, 0.60° ± 0.05 during left stimulation and 0.59° ± 0.11 during stimulation of the right visual field. A two-tailed paired t-test comparing the eye positions during incoherent motion and those observed during the different periods of coherent motion presentation did not reveal any significant difference. For all motion directions considered and all the three different visual stimulation conditions the smallest p value observed was 0.15 for horizontal and 0.07 for vertical eye positions (smallest p: x-axis: $T = 1.46$, $p = 0.15$ for motion in 30° direction (left stimulation); y-axis: $T = -1.82$ $p = 0.07$ for motion in 150° direction during bilateral stimulation). Stable fixation was also observed during retinotopic mapping with the mean eye positions being -0.09° ± 0.57 (horizontal) and -1.14° ± 0.94 (vertical).

Discussion

As suggested by previous work (Braddick et al. 2001; Sunaert et al. 1999), sensitivity to coherent visual motion was not confined to the MT+ complex but was present also in intra-parietal, parieto-occipital and lateral occipital areas. In fact, except for the early visual areas V1–V4 and areas IPS3-5, all the other visual areas responded more strongly to coherent visual motion as compared to motion noise.

By combining visual stimulation with a demanding attention task directed to the central fixation point and by resorting to topographical mapping strategies that have recently been used to characterize cortex along the intra-parietal sulcus (Konen and Kastner 2008; Swisher et al. 2007), we can extend and specify earlier reports on representations of motion coherence in human cerebral cortex. (i) Control of the attentional demands supports the conclusion that stronger responses to coherent motion were not due to differences in attention between conditions. (ii) Definition of the boundaries and spatial representations of topographically-organized cortical areas on a single subject basis allowed for characterizing the responses of these

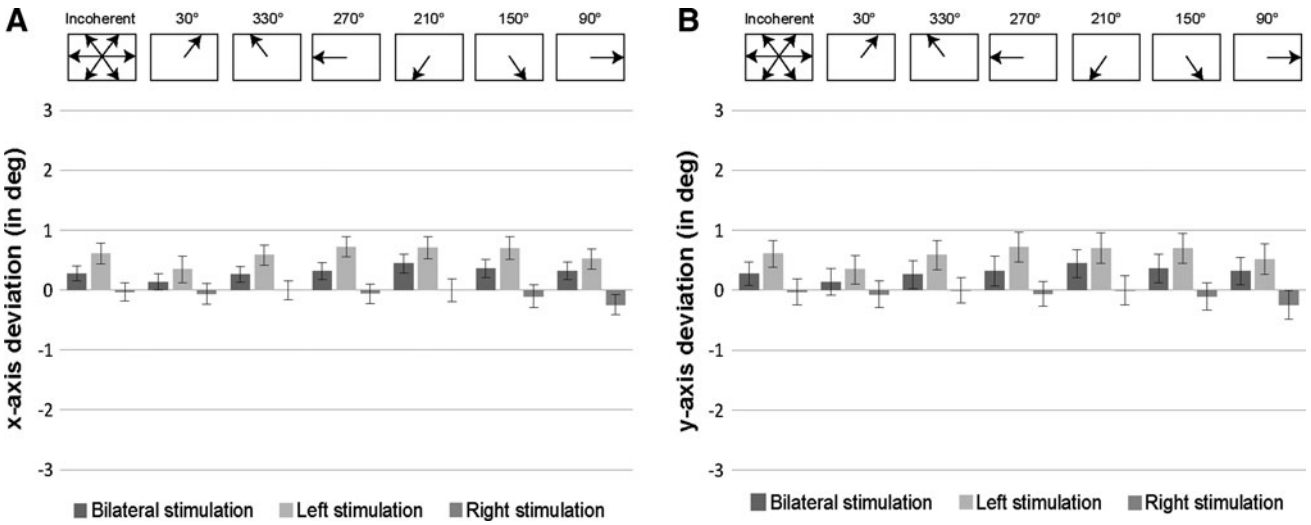

Fig. 8 Eye positions during incoherent motion presentation and during the six different coherent motion conditions (group means and SEM). Horizontal (**a**) and vertical (**b**) eye positions are given for all three stimulation conditions (bilateral, left and right stimulation)

areas independently from the large inter-subject variability with respect to their sizes and locations (Silver and Kastner 2009). The areas showing the most consistent representations of motion coherence across conditions were areas V6, MT/MST, V3A, IPS0-2, and SPL1. (iii) Hemispheric differences were negligible altogether suggesting that asymmetries such as observed in parietal cortex in cognitive tasks do not reflect differences in basic visual response properties. (iv) Comparison of the representations of coherent visual motion between conditions of contralateral and ipsilateral stimulation revealed specialized motion areas that not only indicated coherent motion in the contralateral but also the ipsilateral visual field. In the following we will discuss the different areas representing coherent visual motion with particular emphasis on V6 and the IPS. We will then address the global representation of motion coherence observed in some of these areas.

Across all conditions, area V6 was the region showing the most consistent and strongest response to global visual motion. Specifically, for all three stimulation conditions (ispilateral, contralateral, and bilateral stimulation) V6 revealed the largest effect sizes with respect to visual motion type. This result is completely in line with the recent emphasis on the role of V6 in global visual motion processing (Cardin and Smith 2010; Fattori et al. 2009; Pitzalis et al. 2010; Stenbacka and Vanni 2007). In particular, it confirms the observation of Pitzalis et al. (2010) that V6 showed even higher sensitivity to motion coherence than the MT+ complex. While V6 has been thoroughly described in the macaque (Galletti et al. 1999a; Galletti et al. 2001) the putative human homolog has only been delineated recently (Fattori et al. 2009; Pitzalis et al. 2006; Pitzalis et al. 2010). The region is located in the parieto-occipital sulcus adjacent to area V3A and medial to the intraparietal sulcus. It is possible that it corresponds to area POIPS as addressed by Orban et al. (2006) although this question is not completely resolved (Stiers et al. 2006). Earlier studies have reported activations in medial parieto-occipital cortex to full field visual stimuli correlating with the percept of vection (Brandt et al. 1998; Kovacs et al. 2008a; Kovacs et al. 2008b) or the percept of visual background motion during pursuit eye movements (Haarmeier and Thier 1998; Tikhonov et al. 2004), however, without characterizing this region as a retinotopic representation. In a recent fMRI study, Cardin and Smith (2010) demonstrated that putative V6 preferred flow field stimuli truly simulating ego-motion. The same authors pointed towards some variability of the location of V6, both, between subjects of the same study and also between studies (Pitzalis et al. 2010). The mean Talairach coordinates observed for V6 in this study (Table 1; $x = 20$, $y = -76$, $z = 31$) were in good agreement with the previous studies with a small tendency for a more lateral center of activation ((Pitzalis et al. 2006); $x = 11$, $y = -72$, $z = 46$; (Cardin and Smith 2010), $x = 11$, $y = -79$, $z = 30$). This minor shift along the x-axis is probably the consequence of the smaller stimuli used in our study unable to stimulate the outer eccentricity. The reason is that V6 houses its foveal representation in the most lateral parts of the parieto-occipital sulcus, while the outer eccentricity is represented in the most medial parts. In other words, the smaller the stimulus, the more lateral is the center of activation expected to lie. The specific role of V6 is yet to be defined. In this study, V6 revealed the same functional properties with respect to motion analysis as MST, i.e. a robust preference for coherent motion, not only in the contralateral but also the ipsilateral visual field (see below). The question as to its specific functional role, distinct from area MT/MST, remains an important question for future studies.

Apart from the MT/MST complex and area V6, also areas in the IPS preferred coherent visual motion to motion noise. For contralateral stimulation, four out of seven topographic maps isolated showed this preference, areas IPS0-IPS3 and SPL1. As proposed by Swisher et al. (Swisher et al. 2007; Wandell et al. 2007) we refer to area IPS0 instead of V7 to account for its anatomical location inside the intraparietal sulcus. Areas IPS0-4 have consistently been described in several studies, with IPS0-2 being defined by retinotopic mapping (Konen and Kastner 2008; Silver and Kastner 2009), their anatomical topography and activations during other tasks, such as saccades, selective visual attention and visuospatial motor planning (Hagler et al. 2007; Schluppeck et al. 2006; Schluppeck et al. 2005; Silver et al. 2005). In contrast, IPS3 and IPS4 have usually been described by their visual field maps alone (Konen and Kastner 2008; Swisher et al. 2007; Wandell et al. 2007). IPS5 and SPL1 are again defined by their retinotopic visual representation (Konen and Kastner 2008; Silver and Kastner 2009).

Earlier functional imaging studies reported two motion-responsive clusters within the IPS (Sunaert et al. 1999), a first one located in the occipital IPS (Talairach coordinates by Sunaert et al., 1999; $x = 26$, $y = -76$, $z = 26$) and a second anterior IPS cluster ($x = 30$, $y = -44$, $z = 52$). These coordinates are in good agreement with our locations found for IPS0 ($x = 26$, $y = -77$, $z = 28$) and IPS5 ($x = 32$, $y = -44$, $z = 47$), respectively. Our study suggests a more continuous representation of coherent visual motion along the IPS like shown by Konen and Kastner (2008), however, the small effects in IPS 3–5, which we found during contralateral visual stimulation could not be validated here in the other experiments. In monkey IPS, the area most sensitive to visual motion and flow field information is area VIP which also responds to smooth pursuit eye movements (Cavada 2001; Orban et al. 2006; Schaafsma et al. 1997; Schlack et al. 2003; Vanduffel et al.

2001). The majority of VIP neurons respond both to visual and also tactile stimulation (Colby et al. 1993; Duhamel et al. 1998). The co-registration of tactile and visual spatial maps has also been reported for an area in human superior parietal cortex (Sereno and Huang 2006), and based on topographic organization and anatomical location, this superior parietal area has been suggested to correspond to area IPS5. Other possible human homologs of VIP have also been discussed (Bremmer et al. 2001; Grefkes and Fink 2005; Orban et al. 2006; Orban et al. 2004; Sereno and Tootell 2005; Zhang and Britten 2004; Zhang et al. 2004). The results of this study argue for IPS5 neighboring area SPL1 as the putative homolog of VIP given its preference for global visual motion which, however, was present also in IPS0-2.

In contrast to previous studies which oftentimes have not been able to demonstrate preferences for global visual motion in the MT+ complex (McKeefry et al. 1997; Pitzalis et al. 2010), the present study showed clear representations of global visual motion in the MT+ complex, foremost area MST. This is expected given the decisive evidence for motion integration in MT/MST as derived from numerous monkey experiments (Born and Bradley 2005). Lack of the same features in human experiments is almost certainly a reflection of methodological limitations rather than of qualitative differences between species. In fact, the stimulus configuration used here was chosen to allow for optimal summation within the receptive fields of MST neurons (Becker et al. 2008).

The group of areas revealing coherent visual motion preferences was completed by areas V3A/B and LO1/2, the first described in numerous previous fMRI experiments (Braddick et al. 2001; Nakamura et al. 2001; Press et al. 2001; Sunaert et al. 1999; Vanduffel et al. 2001), and the latter reliably found lateral to intraparietal regions and posterior to the MT+ complex. Areas LO1 and LO2 house two hemifield maps (Larsson and Heeger 2006). They probably include the motion-sensitive area KO (kinetic occipital (Van Oostende et al. 1997)) and are also referred to as the lateral occipital sulcus/complex (LOS/LOC) (Orban et al. 2006; Sunaert et al. 1999). The LOC of macaques is not equivalent to the human LOC, as the lateral occipital cortex of macaques is mostly covered by V1. Since the human LOC lacks a homolog in macaques, the medial occipital cortex of humans has been discussed as a putative functional homolog (Kaido et al. 2004; Larsson and Heeger 2006; Tootell et al. 1998). By dividing the two regions using retinotopic mapping stimuli we found a difference between their responses to global motion with LO1 showing stronger preferences for coherent motion than LO2 which remained significant also for ipsilateral visual motion stimuli.

In primates, it is well accepted that visual input to each cerebral cortical hemisphere comes largely from the contralateral visual hemifield. In macaque monkeys, input to V1 appears almost completely crossed, with missing or only negligible activation from the ipsilateral visual field (Tootell et al. 1998). However, in progressively higher-tier cortical areas, neurons have correspondingly larger receptive fields, including increasing input from the visual field on the same (ipsilateral) side of the brain. Also in this study, significant responses were induced by ipsilateral visual motion stimuli with the most prominent being present in V6, V3A, MST, IPS0 and SPL1. In line with earlier studies (Tootell et al. 1998; Jack et al. 2007), these responses were not observed in early visual cortex but started to emerge in the intermediate areas. Importantly, careful control of eye movements ensured that visual stimuli did not come to lie in both visual hemifields as a consequence of direct fixation of the stimuli. This conclusion was further supported by the fact that responses of V1 to incoherent visual motion, so large under conditions of contralateral stimulation (Fig. 3), were virtually absent when visual stimuli were presented in the ipsilateral field (Fig. 4). Likewise, activations in area MT preferred coherent visual motion only with visual motion in the contralateral visual field, i.e. coherence specificity in MT was confined to contralateral visual motion. These qualitative differences would not have been observed, if the stimuli had encroached significantly on the contralateral field. Ipsilateral responses were, thus, not due to eye movement artifacts but in fact were cortical representations of ipsilateral visual motion. Such activations arguably reflect neurons within these areas that have very large receptive fields owing to callosal inputs that transfer visual information across hemispheres. While this view has been established for MST (Dubner and Zeki 1971; Maunsell and van Essen 1983; Desimone and Ungerleider 1986; Rees et al. 2000; Dukelow et al. 2001; Huk et al. 2002), it may also hold true for the other areas V6, V3A, IPS0 and SPL1. With respect to V6, i.e. the area with the most specific responses to motion coherence in this study, it has indeed been demonstrated in the monkey that the receptive fields cover parts of also the ipsilateral visual field (Galletti et al. 1991). In opposition to this interpretation is our finding that areas which were activated by ipsilateral global motion did not respond to ipsilateral angular mapping stimuli. Quite the contrary, some of these areas in fact were showing negative BOLD responses to ipsilateral angular mapping stimuli (see Fig. 4). This observation suggests that responses to ipsilateral motion were not just due to large receptive fields crossing the vertical meridian but could also be the consequence of backprojections arising from higher-tier cortical areas. In any case, the switch in spatial representation in specialized motion areas from contralateral to global full-field coding defines the cortical

network that has access to the global motion information important for ego-motion perception and navigation.

Acknowledgments The authors are grateful to Rüdiger Berndt and especially Dr. Friedemann Bunjes for their technical assistance. We thank M.B. Wall for his initial remarks on the retinotopic mapping analysis.

References

Allman JM, Kaas JH (1971) Representation of the visual field in striate and adjoining cortex of the owl monkey (*Aotus trivirgatus*). Brain Res 35(1):89–106

Amano K, Wandell BA, Dumoulin SO (2009) Visual field maps, population receptive field sizes, and visual field coverage in the human MT+ complex. J Neurophysiol 102(5):2704–2718

Andersen RA (1989) Visual and eye movement functions of the posterior parietal cortex. Annu Rev Neurosci 12:377–403

Astafiev SV, Shulman GL, Stanley CM, Snyder AZ, Van Essen DC, Corbetta M (2003) Functional organization of human intraparietal and frontal cortex for attending, looking, and pointing. J Neurosci 23(11):4689–4699

Becker HG, Erb M, Haarmeier T (2008) Differential dependency on motion coherence in subregions of the human MT+ complex. Eur J Neurosci 28(8):1674–1685

Born RT, Bradley DC (2005) Structure and function of visual area MT. Annu Rev Neurosci 28:157–189

Braddick OJ, O'Brien JM, Wattam-Bell J, Atkinson J, Hartley T, Turner R (2001) Brain areas sensitive to coherent visual motion. Perception 30(1):61–72

Brandt T, Bartenstein P, Janek A, Dieterich M (1998) Reciprocal inhibitory visual-vestibular interaction. Visual motion stimulation deactivates the parieto-insular vestibular cortex. Brain 121(Pt 9):1749–1758

Bremmer F, Schlack A, Shah NJ, Zafiris O, Kubischik M, Hoffmann K, Zilles K, Fink GR (2001) Polymodal motion processing in posterior parietal and premotor cortex: a human fMRI study strongly implies equivalencies between humans and monkeys. Neuron 29(1):287–296

Cardin V, Smith AT (2010) Sensitivity of human visual and vestibular cortical regions to egomotion-compatible visual stimulation. Cereb Cortex 20(8):1964–1973

Cavada C (2001) The visual parietal areas in the macaque monkey: current structural knowledge and ignorance. Neuroimage 14(1 Pt 2): S21–S26

Cohen J (1988) Statistical power analysis for the behavioral sciences, 2nd edn. Erlbaum, Hillsdale

Colby CL, Duhamel JR, Goldberg ME (1993) The analysis of visual space by the lateral intraparietal area of the monkey: the role of extraretinal signals. Prog Brain Res 95:307–316

Deichmann R, Schwarzbauer C, Turner R (2004) Optimisation of the 3D MDEFT sequence for anatomical brain imaging: technical implications at 1.5 and 3 T. Neuroimage 21(2):757–767

Desimone R, Ungerleider LG (1986) Multiple visual areas in the caudal superior temporal sulcus of the macaque. J Comp Neurol 248(2):164–189

DeYoe EA, Carman GJ, Bandettini P, Glickman S, Wieser J, Cox R, Miller D, Neitz J (1996) Mapping striate and extrastriate visual areas in human cerebral cortex. Proc Natl Acad Sci USA 93(6):2382–2386

Dubner R, Zeki SM (1971) Response properties and receptive fields of cells in an anatomically defined region of the superior temporal sulcus in the monkey. Brain Res 35(2):528–532

Duhamel JR, Colby CL, Goldberg ME (1998) Ventral intraparietal area of the macaque: congruent visual and somatic response properties. J Neurophysiol 79(1):126–136

Dukelow SP, DeSouza JF, Culham JC, van den Berg AV, Menon RS, Vilis T (2001) Distinguishing subregions of the human MT+ complex using visual fields and pursuit eye movements. J Neurophysiol 86(4):1991–2000

Dumoulin SO, Bittar RG, Kabani NJ, Baker CL Jr, Le Goualher G, Bruce Pike G, Evans AC (2000) A new anatomical landmark for reliable identification of human area V5/MT: a quantitative analysis of sulcal patterning. Cereb Cortex 10(5):454–463

Engel SA, Rumelhart DE, Wandell BA, Lee AT, Glover GH, Chichilnisky EJ, Shadlen MN (1994) fMRI of human visual cortex. Nature 369(6481):525

Evangeliou MN, Raos V, Galletti C, Savaki HE (2009) Functional imaging of the parietal cortex during action execution and observation. Cereb Cortex 19(3):624–639

Fattori P, Galletti C, Battaglini PP (1992) Parietal neurons encoding visual space in a head-frame of reference. Boll Soc Ital Biol Sper 68(11):663–670

Fattori P, Pitzalis S, Galletti C (2009) The cortical visual area V6 in macaque and human brains. J Physiol Paris 103(1–2):88–97

Fox PT, Raichle ME (1985) Stimulus rate determines regional brain blood flow in striate cortex. Ann Neurol 17(3):303–305

Galletti C, Battaglini PP, Fattori P (1991) Functional properties of neurons in the anterior bank of the parieto-occipital sulcus of the macaque monkey. Eur J Neurosci 3(5):452–461

Galletti C, Fattori P, Battaglini PP, Shipp S, Zeki S (1996) Functional demarcation of a border between areas V6 and V6A in the superior parietal gyrus of the macaque monkey. Eur J Neurosci 8(1):30–52

Galletti C, Fattori P, Gamberini M, Kutz DF (1999a) The cortical visual area V6: brain location and visual topography. Eur J Neurosci 11(11):3922–3936

Galletti C, Fattori P, Kutz DF, Gamberini M (1999b) Brain location and visual topography of cortical area V6A in the macaque monkey. Eur J Neurosci 11(2):575–582

Galletti C, Gamberini M, Kutz DF, Fattori P, Luppino G, Matelli M (2001) The cortical connections of area V6: an occipito-parietal network processing visual information. Eur J Neurosci 13(8): 1572–1588

Goebel R, Khorram-Sefat D, Muckli L, Hacker H, Singer W (1998) The constructive nature of vision: direct evidence from functional magnetic resonance imaging studies of apparent motion and motion imagery. Eur J Neurosci 10(5):1563–1573

Grefkes C, Fink GR (2005) The functional organization of the intraparietal sulcus in humans and monkeys. J Anat 207(1):3–17

Haarmeier T, Kammer T (2010) Effect of TMS on oculomotor behavior but not perceptual stability during smooth pursuit eye movements. Cereb Cortex 20(9):2234–2243

Haarmeier T, Thier P (1998) An electrophysiological correlate of visual motion awareness in man. J Cogn Neurosci 10(4):464–471

Hagler DJ Jr, Riecke L, Sereno MI (2007) Parietal and superior frontal visuospatial maps activated by pointing and saccades. Neuroimage 35(4):1562–1577

Handel B, Lutzenberger W, Thier P, Haarmeier T (2008) Selective attention increases the dependency of cortical responses on visual motion coherence in man. Cereb Cortex 18(12):2902–2908

Heide W, Kompf D (1998) Combined deficits of saccades and visuospatial orientation after cortical lesions. Exp Brain Res 123(1–2): 164–171

Huk AC, Dougherty RF, Heeger DJ (2002) Retinotopy and functional subdivision of human areas MT and MST. J Neurosci 22(16): 7195–7205

Jack AI, Patel GH, Astafiev SV, Snyder AZ, Akbudak E, Shulman GL, Corbetta M (2007) Changing human visual field

organization from early visual to extra-occipital cortex. PLoS ONE 2(5):e452
Kaido T, Hoshida T, Taoka T, Sakaki T (2004) Retinotopy with coordinates of lateral occipital cortex in humans. J Neurosurg 101(1):114–118
Kolster H, Peeters R, Orban GA (2010) The retinotopic organization of the human middle temporal area MT/V5 and its cortical neighbors. J Neurosci 30(29):9801–9820
Konen CS, Kastner S (2008) Representation of eye movements and stimulus motion in topographically organized areas of human posterior parietal cortex. J Neurosci 28(33):8361–8375
Kovacs G, Cziraki C, Vidnyanszky Z, Schweinberger SR, Greenlee MW (2008a) Position-specific and position-invariant face aftereffects reflect the adaptation of different cortical areas. Neuroimage 43(1):156–164
Kovacs G, Raabe M, Greenlee MW (2008b) Neural correlates of visually induced self-motion illusion in depth. Cereb Cortex 18(8):1779–1787
Larsson J, Heeger DJ (2006) Two retinotopic visual areas in human lateral occipital cortex. J Neurosci 26(51):13128–13142
Larsson J, Landy MS, Heeger DJ (2006) Orientation-selective adaptation to first- and second-order patterns in human visual cortex. J Neurophysiol 95(2): 862–881
Maunsell JH, van Essen DC (1983) The connections of the middle temporal visual area (MT) and their relationship to a cortical hierarchy in the macaque monkey. J Neurosci 3(12):2563–2586
McKeefry DJ, Watson JD, Frackowiak RS, Fong K, Zeki S (1997) The activity in human areas V1/V2, V3, and V5 during the perception of coherent and incoherent motion. Neuroimage 5(1):1–12
Nakamura H, Kuroda T, Wakita M, Kusunoki M, Kato A, Mikami A, Sakata H, Itoh K (2001) From three-dimensional space vision to prehensile hand movements: the lateral intraparietal area links the area V3A and the anterior intraparietal area in macaques. J Neurosci 21(20):8174–8187
Oldfield RC (1971) The assessment and analysis of handedness: the Edinburgh inventory. Neuropsychologia 9(1):97–113
Orban GA, Van Essen D, Vanduffel W (2004) Comparative mapping of higher visual areas in monkeys and humans. Trends Cogn Sci 8(7):315–324
Orban GA, Claeys K, Nelissen K, Smans R, Sunaert S, Todd JT, Wardak C, Durand JB, Vanduffel W (2006) Mapping the parietal cortex of human and non-human primates. Neuropsychologia 44(13):2647–2667
Pitzalis S, Galletti C, Huang RS, Patria F, Committeri G, Galati G, Fattori P, Sereno MI (2006) Wide-field retinotopy defines human cortical visual area v6. J Neurosci 26(30):7962–7973
Pitzalis S, Sereno MI, Committeri G, Fattori P, Galati G, Patria F, Galletti C (2010) Human v6: the medial motion area. Cereb Cortex 20(2):411–424
Posner MI, Petersen SE (1990) The attention system of the human brain. Annu Rev Neurosci 13:25–42
Press WA, Brewer AA, Dougherty RF, Wade AR, Wandell BA (2001) Visual areas and spatial summation in human visual cortex. Vis Res 41(10–11):1321–1332
Rees G, Friston K, Koch C (2000) A direct quantitative relationship between the functional properties of human and macaque V5. Nat Neurosci 3(7):716–723
Schaafsma SJ, Duysens J, Gielen CC (1997) Responses in ventral intraparietal area of awake macaque monkey to optic flow patterns corresponding to rotation of planes in depth can be explained by translation and expansion effects. Vis Neurosci 14(4):633–646
Schlack A, Hoffmann KP, Bremmer F (2003) Selectivity of macaque ventral intraparietal area (area VIP) for smooth pursuit eye movements. J Physiol 551(Pt 2):551–561
Schluppeck D, Glimcher P, Heeger DJ (2005) Topographic organization for delayed saccades in human posterior parietal cortex. J Neurophysiol 94(2):1372–1384
Schluppeck D, Curtis CE, Glimcher PW, Heeger DJ (2006) Sustained activity in topographic areas of human posterior parietal cortex during memory-guided saccades. J Neurosci 26(19):5098–5108
Sereno MI, Huang RS (2006) A human parietal face area contains aligned head-centered visual and tactile maps. Nat Neurosci 9(10):1337–1343
Sereno MI, Tootell RB (2005) From monkeys to humans: what do we now know about brain homologies? Curr Opin Neurobiol 15(2):135–144
Sereno MI, Dale AM, Reppas JB, Kwong KK, Belliveau JW, Brady TJ, Rosen BR, Tootell RB (1995) Borders of multiple visual areas in humans revealed by functional magnetic resonance imaging. Science 268(5212):889–893
Sereno MI, Pitzalis S, Martinez A (2001) Mapping of contralateral space in retinotopic coordinates by a parietal cortical area in humans. Science 294(5545):1350–1354
Sheremata SL, Bettencourt KC, Somers DC (2010) Hemispheric asymmetry in visuotopic posterior parietal cortex emerges with visual short-term memory load. J Neurosci 30(38):12581–12588
Silver MA, Kastner S (2009) Topographic maps in human frontal and parietal cortex. Trends Cogn Sci 13(11):488–495
Silver MA, Ress D, Heeger DJ (2005) Topographic maps of visual spatial attention in human parietal cortex. J Neurophysiol 94(2):1358–1371
Smith AT, Greenlee MW, Singh KD, Kraemer FM, Hennig J (1998) The processing of first- and second-order motion in human visual cortex assessed by functional magnetic resonance imaging (fMRI). J Neurosci 18(10):3816–3830
Smith AT, Wall MB, Williams AL, Singh KD (2006) Sensitivity to optic flow in human cortical areas MT and MST. Eur J Neurosci 23(2):561–569
Stenbacka L, Vanni S (2007) fMRI of peripheral visual field representation. Clin Neurophysiol 118(6):1303–1314
Stiers P, Peeters R, Lagae L, Van Hecke P, Sunaert S (2006) Mapping multiple visual areas in the human brain with a short fMRI sequence. Neuroimage 29(1):74–89
Sunaert S, Van Hecke P, Marchal G, Orban GA (1999) Motion-responsive regions of the human brain. Exp Brain Res 127(4): 355–370
Swisher JD, Halko MA, Merabet LB, McMains SA, Somers DC (2007) Visual topography of human intraparietal sulcus. J Neurosci 27(20):5326–5337
Talairach J, Tournoux P (1988) Co-planar stereotaxic atlas of the human brain. 3-Dimensional proportional system: an approach to cerebral imaging. Thieme, New York, NY, USA
Tikhonov A, Haarmeier T, Thier P, Braun C, Lutzenberger W (2004) Neuromagnetic activity in medial parietooccipital cortex reflects the perception of visual motion during eye movements. Neuroimage 21(2):593–600
Tootell RB, Reppas JB, Dale AM, Look RB, Sereno MI, Malach R, Brady TJ, Rosen BR (1995) Visual motion aftereffect in human cortical area MT revealed by functional magnetic resonance imaging. Nature 375(6527):139–141
Tootell RB, Mendola JD, Hadjikhani NK, Ledden PJ, Liu AK, Reppas JB, Sereno MI, Dale AM (1997) Functional analysis of V3A and related areas in human visual cortex. J Neurosci 17(18):7060–7078
Tootell RB, Mendola JD, Hadjikhani NK, Liu AK, Dale AM (1998) The representation of the ipsilateral visual field in human cerebral cortex. Proc Natl Acad Sci USA 95(3):818–824
Van Oostende S, Sunaert S, Van Hecke P, Marchal G, Orban GA (1997) The kinetic occipital (KO) region in man: an fMRI study. Cereb Cortex 7(7):690–701

Vanduffel W, Fize D, Mandeville JB, Nelissen K, Van Hecke P, Rosen BR, Tootell RB, Orban GA (2001) Visual motion processing investigated using contrast agent-enhanced fMRI in awake behaving monkeys. Neuron 32(4):565–577

von Pfostl V, Stenbacka L, Vanni S, Parkkonen L, Galletti C, Fattori P (2009) Motion sensitivity of human V6: a magnetoencephalography study. Neuroimage 45(4):1253–1263

Wade AR, Brewer AA, Rieger JW, Wandell BA (2002) Functional measurements of human ventral occipital cortex: retinotopy and colour. Philos Trans R Soc Lond B Biol Sci 357(1424):963–973

Wall MB, Lingnau A, Ashida H, Smith AT (2008) Selective visual responses to expansion and rotation in the human MT complex revealed by functional magnetic resonance imaging adaptation. Eur J Neurosci 27(10):2747–2757

Wandell BA, Dumoulin SO, Brewer AA (2007) Visual field maps in human cortex. Neuron 56(2):366–383

Zhang T, Britten KH (2004) Clustering of selectivity for optic flow in the ventral intraparietal area. NeuroReport 15(12):1941–1945

Zhang T, Heuer HW, Britten KH (2004) Parietal area VIP neuronal responses to heading stimuli are encoded in head-centered coordinates. Neuron 42(6):993–1001